CONF-781034--1

PREPRINT UCRL- 80256 Rev. I

Lawrence Livermore Laboratory

A Method For Determining the Work Hardening Function To Describe Plasticity of Metals*

Mark L. Wilkins

April 17, 1978

This paper was prepared for the TMS-AIME Shaping and Forming Committee and The AMS Flow and Fracture Committee Symposium: Formability; Analysis, Modeling and Experimentation. October 24,25, 1977, Chicago, Ill

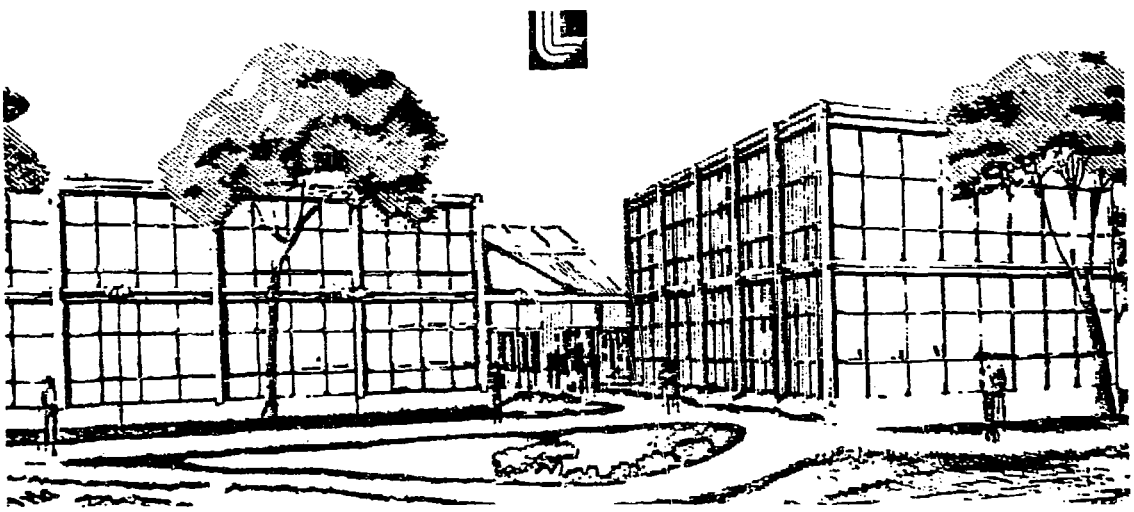

A METHOD FOR DETERMINING THE WORK HARDENING FUNCTION TO DESCRIBE PLASTICITY OF METALS*

Mark L. Wilkins

University of California Lawrence Livermore Laboratory
Livermore, California 94550

The object of this study is to develop a method for obtaining a constitutive relation that relates the flow stress to the equivalent plastic strain. The method uses simple tension test data to suggest a functional form. This form is then used as a constitutive model in a computer program that simulates the tension test. The calculated results are compared with the experimental results and the functional form is refined until agreement is obtained between calculations and experiments. The importance of knowing the relationship between the flow stress and the plastic strain is discussed. A work hardening function is calibrated for 6061 T6 aluminum.

Introduction

Constitutive equations that describe the outstanding features of real phenomena provide models of material behavior that permit calculations of a physical event to be carried to late stages. For example, in the study of spall it is important to know the shape of a stress wave induced in a material in order to calculate the states of stress and strain when the wave interacts with a free boundary. A constitutive relation that adequately describes the evolution of a stress wave progressing in a given material provides the important input to the spall problem, even though details of microscopic phenomena that are responsible for the wave shape may be unknown.

A constitutive equation is a model based on judgment; it is especially useful when it provides a wide-range description. Three fundamental types of mechanical behavior can be associated with the real materials: elasticity, plasticity, and possible rate effects including viscosity. In the engineering application of metals to structural design elastic plastic properties are the main concern.

*W ices of the U.S.D.O.E. under contract W- "Work performed under the auspices of the U.S. Department of Energy by the Lawrence Livermore Laboratory under contract number W-7405-ENG-48."

Elastic-plastic theory has been very successful in describing the behavior of metals and provides a good framework to build models of material behavior. In elastic-plastic theory the total stress is composed of a hydrostatic component, P, and a deviatoric component, s, where a limit is imposed on the magnitude of the deviatoric stress by the yield condition. Constitutive relations for elastic-plastic theory are given by the following equations.

Constitutive Relations

Stress (Hooke's Law):

a) $\dot{s}_{ij} = 2\mu\dot{\varepsilon}_{ij} + \dot{\delta}_{ij}$

b) $\dot{\sigma}_{ij} = -\dot{P} + \dot{s}_{ij}$ for $i = j$ $\qquad i, j = 1, 2, 3.$

c) $\dot{\sigma}_{ij} = \dot{s}_{ij}$ for $i \neq j$

d) $-P = K\dot{V}/V$

Here $\dot{\varepsilon}_{ij}$ is the strain rate deviator, V the volume, μ the shear modulus, K the bulk modulus and $\dot{\delta}_{ij}$ represents a correction term for rigid rotation. The dot over a parameter means a time derivative along a particle path. The time derivative provides a desired ordered sequence for the incremental stress strain relationship and no rate dependent behavior is meant.

Von Mises Yield Condition

$$\sigma_{eq} - Y \leq 0$$

σ_{eq} = equivalent stress $= \sqrt{\frac{3}{2}}\sqrt{2J}$

Y = flow stress $= H(\bar{\varepsilon}^p)$

Here 2J is the second invariant of the deviatoric stress tensor. The total strains are assumed to be the sum of elastic and plastic components. Implicit in this formulation is the sum of the plastic strains is zero (plastic incompressibility). The equivalent plastic strain, $\bar{\varepsilon}^p$, is obtained by integrating during plastic deformation the integral:

$$\bar{\varepsilon}^p = \int d\bar{\varepsilon} \quad \text{where} \quad d\bar{\varepsilon} = \sqrt{\frac{2}{3} d\varepsilon_{ij} d\varepsilon_{ij}}$$

here ε_{ij} are components of the plastic strain.

In satisfying the Von Mises condition the plastic strain rate vector associated with a principal stress vector must be directed outwards along the normal to the yield surface. Computer simulation programs that incorporate the above model of elastic-plastic flow are described in Refs. 1 and 2.

The shear modulus, μ, and bulk modulus, K, can be obtained from ultrasonic measurements. Knowledge of the work hardening function $H(\bar{\varepsilon}^p)$ is

necessary for solutions of problems where plastic deformation occurs (3). The method for obtaining this function for 6061 T6 aluminum is described later.

Importance of the Plastic Work Hardening Function

For the optimum use of materials in an engineering structure, a description is required of the material behavior after the elastic limit has been exceeded. Once provided with the knowledge of the material behavior in the plastic regime, it becomes possible to design with plasticity. An objective might be to find the design that best utilizes material properties by balancing the flow stress and the elongation behavior so that the best economy of materials can be attained. Another objective might be to perform destructive testing on a computer rather than on the physical object.

The great uncertainty in designing with plasticity is to know under what conditions ductile fracture occurs. For example, it is known that elongation to fracture differs according to the combination of stresses occurring during the loading history of the material. The constitutive model for predicting ductile fracture would be expected to be complex and could only come from a calculational and experimental program. The first requirement for studying ductile fracture is knowledge of the plastic work hardening function. With this information the correct stress-strain conditions just prior to fracture can be calculated for experiments where fracture occurs from varying loading histories.

A Method for Determining the Plastic Work Hardening Function

Tension Test

The simple tension test of a cylindrical specimen offers a direct method for relating the equivalent stress, σ_{eq}, to the equivalent plastic strain, $\bar{\varepsilon}^p$. For this test the equivalent stress coincides with the uniaxial stress, σ_{zz}, and the equivalent strain coincides with the extension in the pulling direction. Very large plastic strains can be made to occur in a local region when a ductile cylinder is pulled in tension. A slight taper is used in the cylinder specimen to control the position of the large strains; the smallest diameter being located at the mid-section. The geometry lends itself to very easy measurements of the equivalent stress and equivalent strain.

Stresses

The uniaxial stress is taken as the load divided by the area at the mid-section and is usually called the true stress, σ_T. Thus the proposition is:

$$\sigma_{zz} = \sigma_T = \sigma_{eq}$$

This is only strictly true before the elastic limit has been reached and the axial stress σ_{zz} is uniform across a section of the cylinder. As the plastic strain increases, σ_{zz} and σ_{eq} become increasingly nonuniform.

It is instructive to review the definitions of the axial and equivalent stresses. For the geometry of the tension test the mid-section is a plane of symmetry and the coordinate axes are the principal axes. The second invariant of the deviatoric stress tensor, 2J, can be evaluated from the principal deviatoric stresses:

$$2J = s_{zz}^2 + s_{rr}^2 + s_{\theta\theta}^2$$

The radial and hoop strains are the same, thus $s_{rr} = s_{\theta\theta}$. Since $(s_{zz} + s_{rr} + s_{\theta\theta}) = 0$, $s_{zz} = -2s_{rr}$.

Thus $$2J = \frac{3}{2} s_{zz}^2$$

and

$$\sigma_{eq} = \sqrt{\frac{3}{2}}\sqrt{2J} = \frac{3}{2} s_{zz}$$

The uniaxial stress is: $\sigma_{zz} = -P + s_{zz}$. The radial stress σ_{rr} must be zero at the cylinder free surface, i.e. $\sigma_{rr} = -P + s_{rr} = 0$. Thus

$$P = s_{rr} = -\frac{1}{2} s_{zz}$$

and $\sigma_{zz} = -P + s_{zz} = \frac{3}{2} s_{zz} = \sigma_{eq}$. This of course is not a result but rather, the basis for the original proposition.

After the elastic limit is reached and the tension load on the cylinder continues, the stresses depart from a uniform distribution. This is the region of interest where plastic flow is occurring. The analysis of the experimental results of a tension test assumes that the average uniaxial stress, $\bar{\sigma}_{zz}$, and the average equivalent stress, $\bar{\sigma}_{eq}$, equal the true stress, σ_T.

$$\bar{\sigma}_{zz} = \frac{2}{R^2}\int_{r=0}^{r=R} \sigma_{zz}(r)\, r\, dr = \bar{\sigma}_{eq} = \frac{2}{R^2}\int_{r=0}^{r=R} \sigma_{eq}(r)\, r\, dr = \sigma_T = \frac{\text{LOAD}}{\pi R^2}$$

Here, R is the current outside radius of the cylinder.

The elastic limit is reached first at the mid-section where the cross-sectional area, πR^2, is smallest and hence the stresses the largest. The flow stress, Y, at the mid-section increases when plastic flow occurs. Positions adjacent to the mid-section reach the elastic limit and the process continues until plastic flow extends throughout the specimen length.

The magnitude of the plastic strain in the axial direction falls off as the axial distance from the mid-section increases. A strain measurement must be taken over a region where the strain is constant for the results to be independent of the gage length. In the tension test the strain in the radial direction remains fairly constant even for large plastic deformations. The radial strain can be obtained by measuring the change in diameter of the mid-section. Thus the diameter of the cylinder serves as the gage length. We wish to obtain the strain in the axial

direction and specifically the equivalent plastic strain, $\bar{\varepsilon}^p$. The simple analysis that follows shows the relationship between external measurements and strains in a cylinder.

Strains

External measurements of the radius, R, and an arbitrary axial length, L, taken at the mid-plane of a cylinder can be used to determine the average natural strains:

$$\varepsilon_{zz} = \int_{L^0}^{L} \frac{dL}{L} = \text{Ln}\,\frac{L}{L^0} \qquad \text{axial strain}$$

$$\varepsilon_{rr} = \int_{R^0}^{R} \frac{dR}{R} = \text{Ln}\,\frac{R}{R^0} \qquad \text{radial strain}$$

$$\varepsilon_{\theta\theta} = \int \frac{dR d\theta}{R d\theta} = \int_{R^0}^{R} \frac{dR}{R} = \text{Ln}\,\frac{R}{R^0} \qquad \text{hoop strain}$$

Here L^0 and R^0 are initial dimensions.

The strain $\varepsilon_{\theta\theta}$ is the result of the change in length of a lineal element in the θ-direction where the change in length is due to a displacement in the r-direction. The concept of natural strain compares the extension of an element of length to the current length rather than the initial length.

The volumetric strain, $\int \frac{dv}{v}$, is:

$$\int \frac{dv}{v} = \int \frac{dL}{L} + 2\int \frac{dR}{R}$$

Hence, $\frac{v}{v^0} = \frac{L}{L^0}\left(\frac{R}{R^0}\right)^2$ where v^0 is the initial volume.

The strains ε_{zz}, ε_{rr} and $\varepsilon_{\theta\theta}$ include both elastic, ${}^e\varepsilon$, and plastic, ${}^p\varepsilon$, components i.e. $\varepsilon_{zz} = {}^e\varepsilon_{zz} + {}^p\varepsilon_{zz}$, etc. The elastic components are small compared to the plastic components. (See the analysis of a tension test in Ref. 4.)

It is experimentally observed that the volume doesn't change during plastic flow (plastic incompressibility). Thus if ${}^p\varepsilon_{zz}$, ${}^p\varepsilon_{rr}$, and ${}^p\varepsilon_{\theta\theta}$ are the plastic strains, then,

$${}^p\varepsilon_{zz} + {}^p\varepsilon_{rr} + {}^p\varepsilon_{\theta\theta} = 0$$

Here the plastic strains ${}^p\varepsilon_{zz}$, ${}^p\varepsilon_{rr}$ and ${}^p\varepsilon_{\theta\theta}$ are also the principal plastic strains. The equivalent plastic strain, $\bar{\varepsilon}^p$, for this case is given by:

$$\bar{\varepsilon}^p = \sqrt{\frac{2}{3}}\sqrt{(^p\varepsilon_{zz} - {}^p\varepsilon_{rr})^2 + (^p\varepsilon_{rr} - {}^p\varepsilon_{\theta\theta})^2 + (^p\varepsilon_{\theta\theta} - {}^p\varepsilon_{zz})^2}$$

with $^p\varepsilon_{zz} = -2\,{}^p\varepsilon_{rr} = -2\varepsilon_{\theta\theta}$ the equivalent plastic strain is the axial plastic strain, i.e. $\bar{\varepsilon}^p = {}^p\varepsilon_{zz}$.

Application to 6061-T6 Aluminum

Figure 1 gives experimental results for two aluminum tensile specimens. The same data are shown as load and true stress, σ_T, vs radial strain ε_{rr}. When the data are plotted as ln σ_T vs ln ε_{rr} a straight line is obtained. Thus the data fit the form $\sigma_T = a(\varepsilon_{zz})^n$ where $\varepsilon_{zz} = -2\varepsilon_{rr} = -2$ Ln D/D_0 and D is the cylinder diameter. A convenient form to express the flow stress is $Y = a(b+\bar{\varepsilon}^p)^n$. Here Y has replaced σ_T and $(b+\bar{\varepsilon}^p)$ has replaced ε_{zz} in the relation $\sigma_T = a(\varepsilon_{zz})^n$. The assumption here is that the average stress strain data obtained experimentally can be used to suggest a relation for a point function flow stress. The parameter b could be considered the elastic strain since the experimental strain, $\varepsilon_{zz} = -2$ Ln D/D_0, includes the elastic strain. The elastic strain of course will change as the load changes. Since the components of elastic strains are small compared to the plastic strains we will ignore them and consider b an empirical constant of the order of the strain at the elastic limit. It can be easily shown that with this form for the flow stress the exponent n corresponds to the axial strain at maximum load. Figure 1 shows that this occurs at a radial strain of -0.05, or an axial strain of 0.1. It is of course important that fracture has not occurred in the region of the experimental data used to develop the plasticity function. Fracture of these tensile specimens originates at the center of the specimen. Examination of interrupted tests established that fracture initiates after the peak load when the radial strain is approximately 0.26.

From the load vs radial strain curve the elastic limit is estimated to be 2.85 kb. This is also consistent with Hugoniot elastic limit results that measure the elastic limit in compression. With the constants a and b adjusted to give the flow stress at the elastic limit with n = 0.1, the tension test can be simulated with the HEMP computer program.(1)

Calculations

The HEMP finite difference program (1) used to simulate the tension test solves the equations of continuum mechanics in two space dimensions and time. At each grid point the incremental stress is obtained from strain increments which in turn are obtained from gradients of the velocity field. The constitutive model described earlier was used with the bulk modulus K = 728 kb, the shear modulus, μ = 277kb and the density ρ_0 = 2.703 gm/cc. The initial Lagrange grid was square with 20 grid zones in the radial direction. A fixed axial velocity was applied to the cylinder end. Symmetry boundary conditions were applied at the position corresponding to the midsection of the experimental cylinder which had a 1/2% taper. The program solves the constitutive equations at each zone at discrete time steps. The components of plastic strain are obtained by subtracting from the total strains the elastic strains which are obtained from the stress deviators. This procedure implicitly introduces plastic

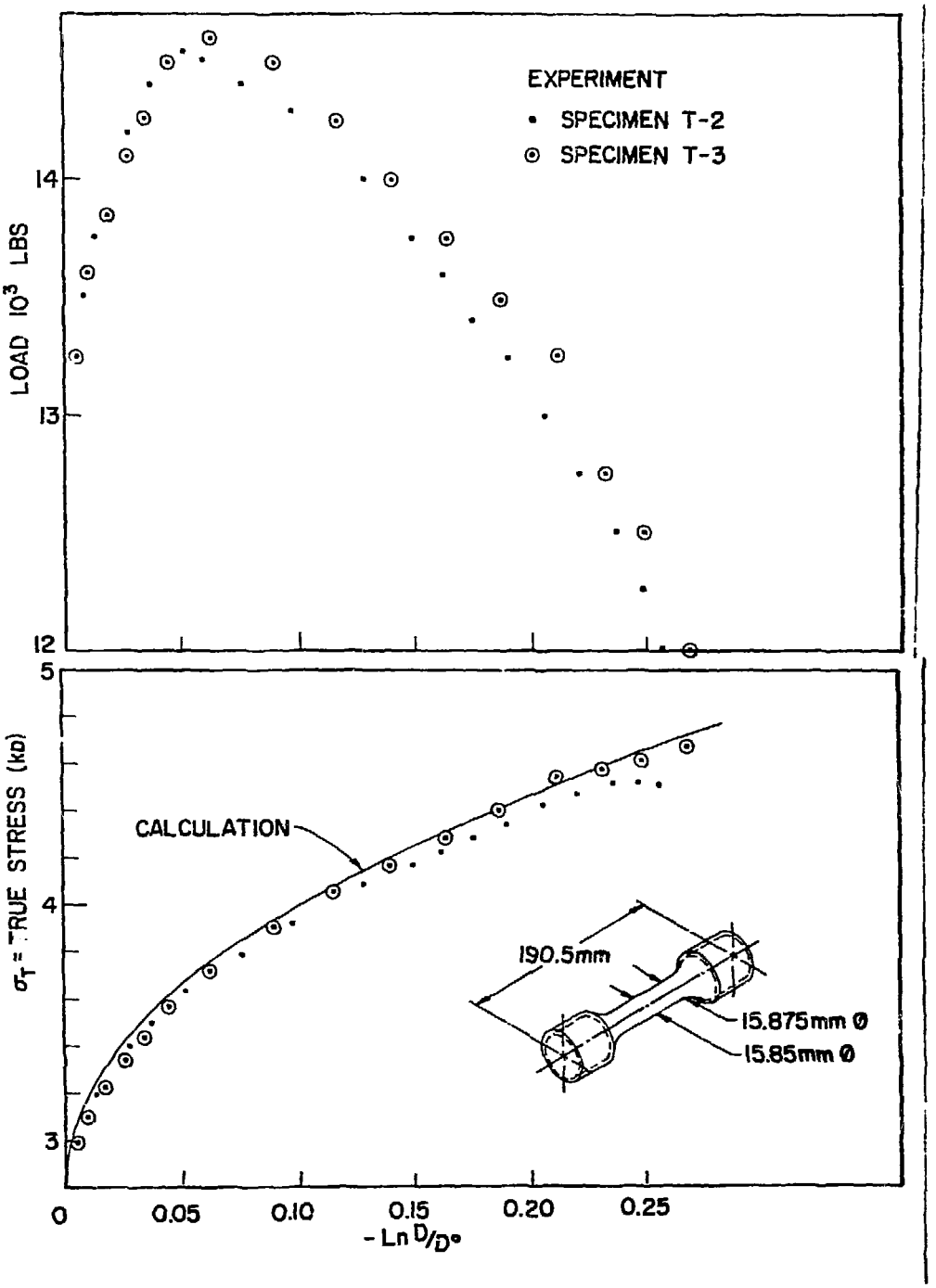

Figure 1 Load and true stress-vs-strain at mid-section of a cylinder pulled in tension, original diameter D^o = 15.85 mm.

incompressibility into the model. The equivalent plastic strain $\bar{\varepsilon}^p$ is evaluated at each zone and is used to calculate the flow stress, $Y = a(b + \bar{\varepsilon}^p)^n$, for the zone. Thus, as mentioned earlier, the average stress strain behavior of the cylinder, obtained from external measurements, is used to suggest a point function flow stress.

Figure 1 shows a comparison of the HEMP calculation with the experiment where a = 4.6, b = 0.008 and n = 0.1 where the flow stress Y is in kb. The calculated true stress shown in Fig. 1 is the axial stress $\bar{\sigma}_{zz}$ described earlier.

Figures 2, 3, and 4 show calculated profiles at the mid-section of the specimen when $R/R^o = 0.772$, the strain just prior to the observed fracture. The stress profiles are not constant. However, it is noted in Fig. 2 that the equivalent plastic strain profile is fairly flat and that the strain calculated from the external radius, $-2 \text{ Ln } R/R^o = -2 \text{ Ln } .772 = 0.52$, is a good measure of the average value of $\bar{\varepsilon}^p$.

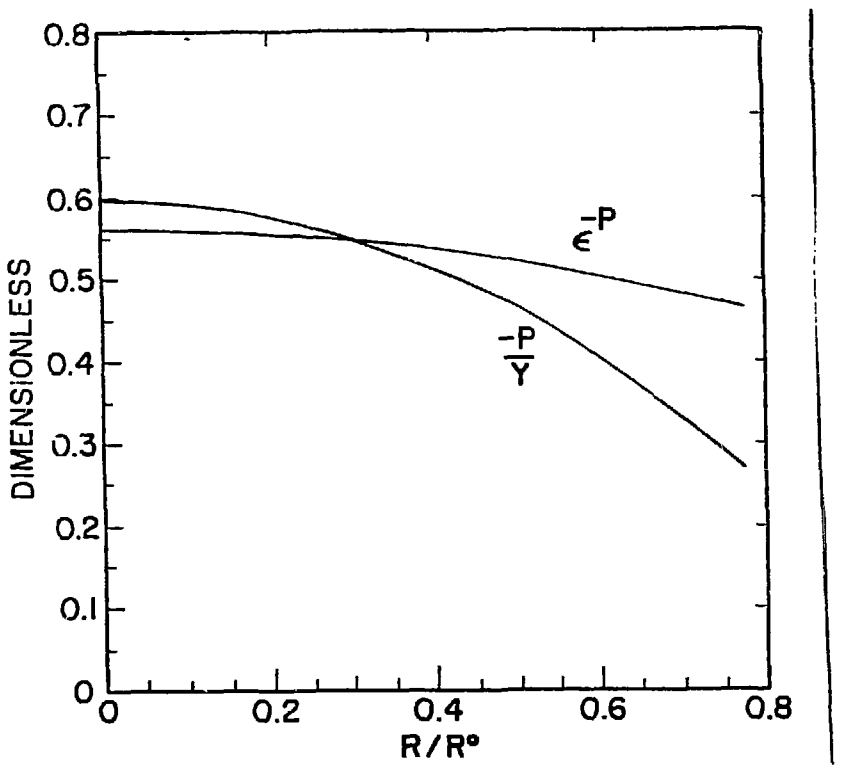

Figure 2 Calculated profiles at the cylinder mid-section at time of fracture, $R/R^o = 0.772$. $\bar{\varepsilon}^p$ is the equivalent plastic strain, $-P/Y$ is the ratio of the hydrostatic stress to the flow stress.

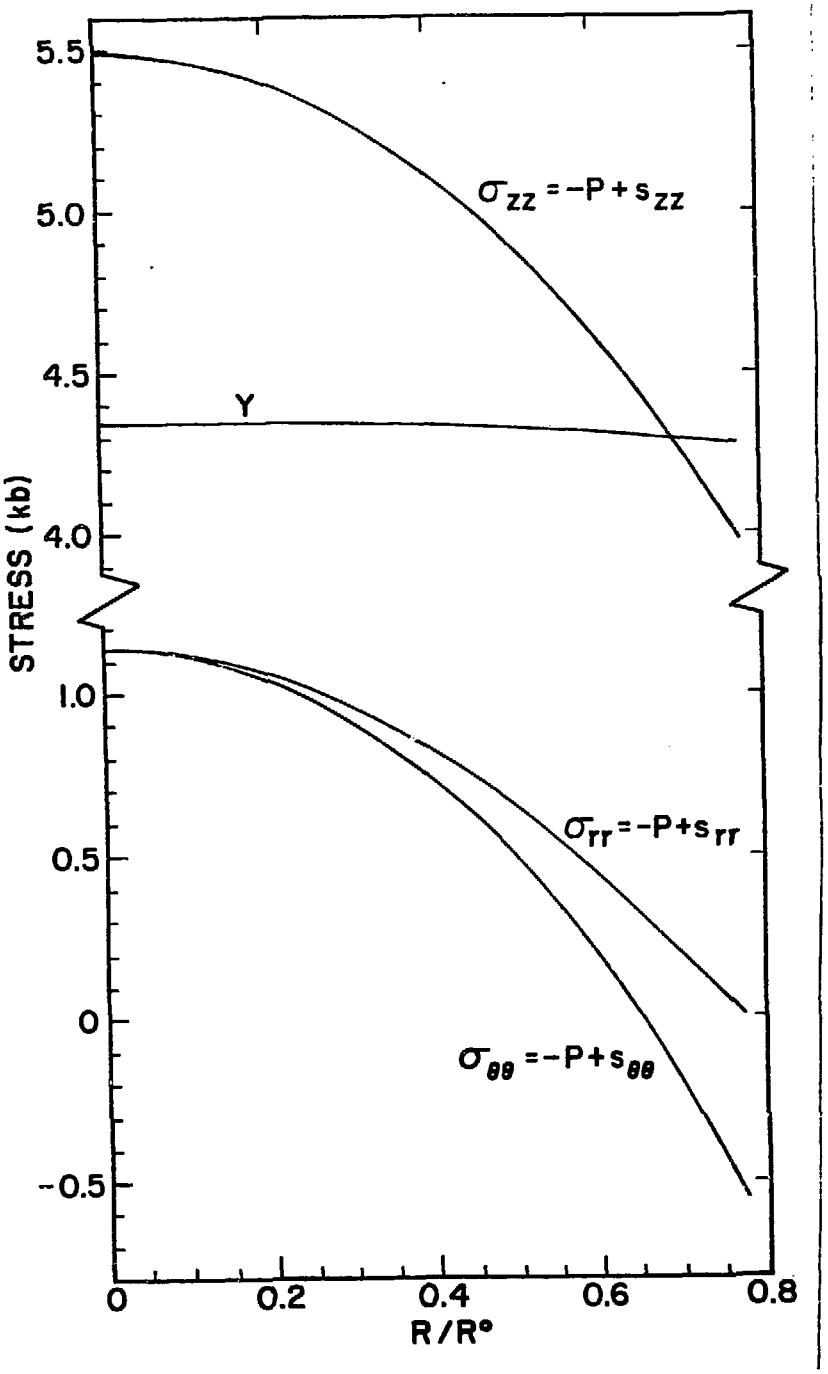

Figure 3 Continued from Figure 2, σ_{zz} is the axial stress, σ_{rr} the radial stress and $\sigma_{\theta\theta}$ the hoop stress. The flow stress Y is also the equivalent stress σ_{eq} since the material is at the elastic limit.

In Fig. 3 it is seen that the axial stress, σ_{zz}, which carries the load, is quite different from the equivalent stress σ_{eq} shown as Y in Fig. 3. The true stress from the simulation program, $\bar{\sigma}_{zz}$, was calculated by summing zone by zone the product of the zone stress and zone area at the mid-plane and dividing by the mid-plane area. The calculated value of the true stress corresponding to Fig. 3 is $\bar{\sigma}_{zz}$ = 4.6 kb which is not too different from a mean value of the equivalent stress, σ_{eq} taken as 4.3 kb, where σ_{eq} = Y. Thus the external measurements on a tension test can give stress strain information suitable for establishing a first guess for a constitutive relation for the plastic work hardening function.

In Fig. 4 it is seen that the hydrostatic stresses , -P, is responsible for the non uniform axial stress, σ_{zz}, in Fig. 3.

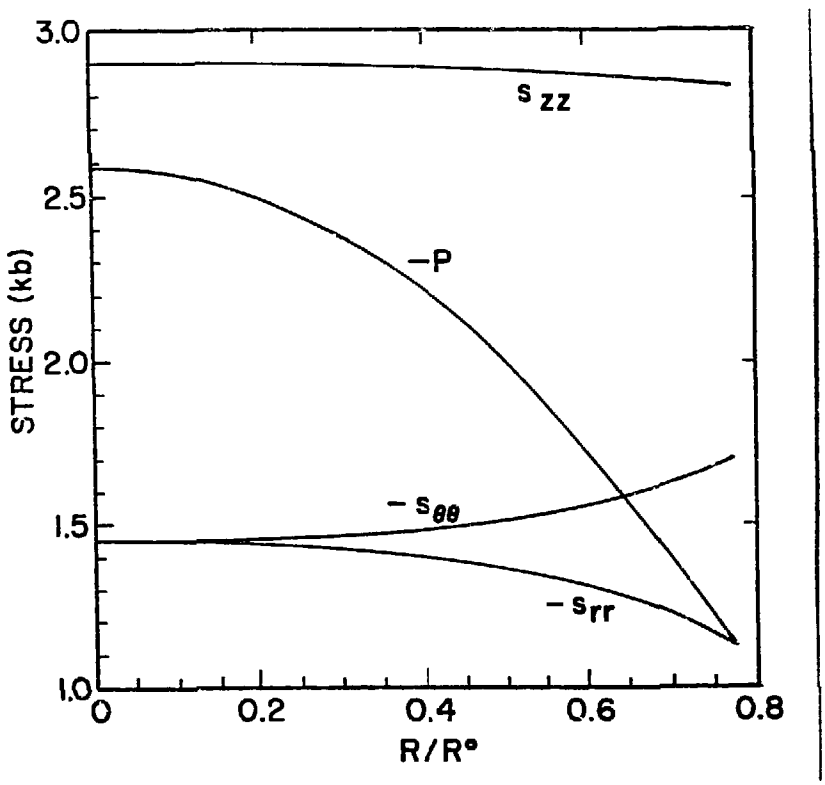

Figure 4 Continued from Figure 2. s_{zz}, s_{rr} and $s_{\theta\theta}$ are stress deviators. -P is the hydrostatic stress.

For aluminum the power law form describes the real phenomena very well and the constants were determined on the first try. For a metal with a more complex work hardening behavior it would be expected that several iterations of the computer simulation program would be necessary to develop a satisfactory form to describe the flow stress (5).

Figures 5 and 6 show contours of the axial stress, σ_{zz}, and the hydrostatic pressure P at the same radial strain as Figs. 2, 3, and 4. It is noted in Fig. 6 that the pressure is compressive in a region one to two radii away from the center. This result is due to the free surface boundary conditions on the exterior of the cylinder. The interior stress in the direction normal to the cylinder free surface must be zero at the free surface. To maintain this stress free condition there is motion normal to the free surface as the cylinder is elongated. The net effect is for material to move away from the center region similar to an extrusion process by squeezing.

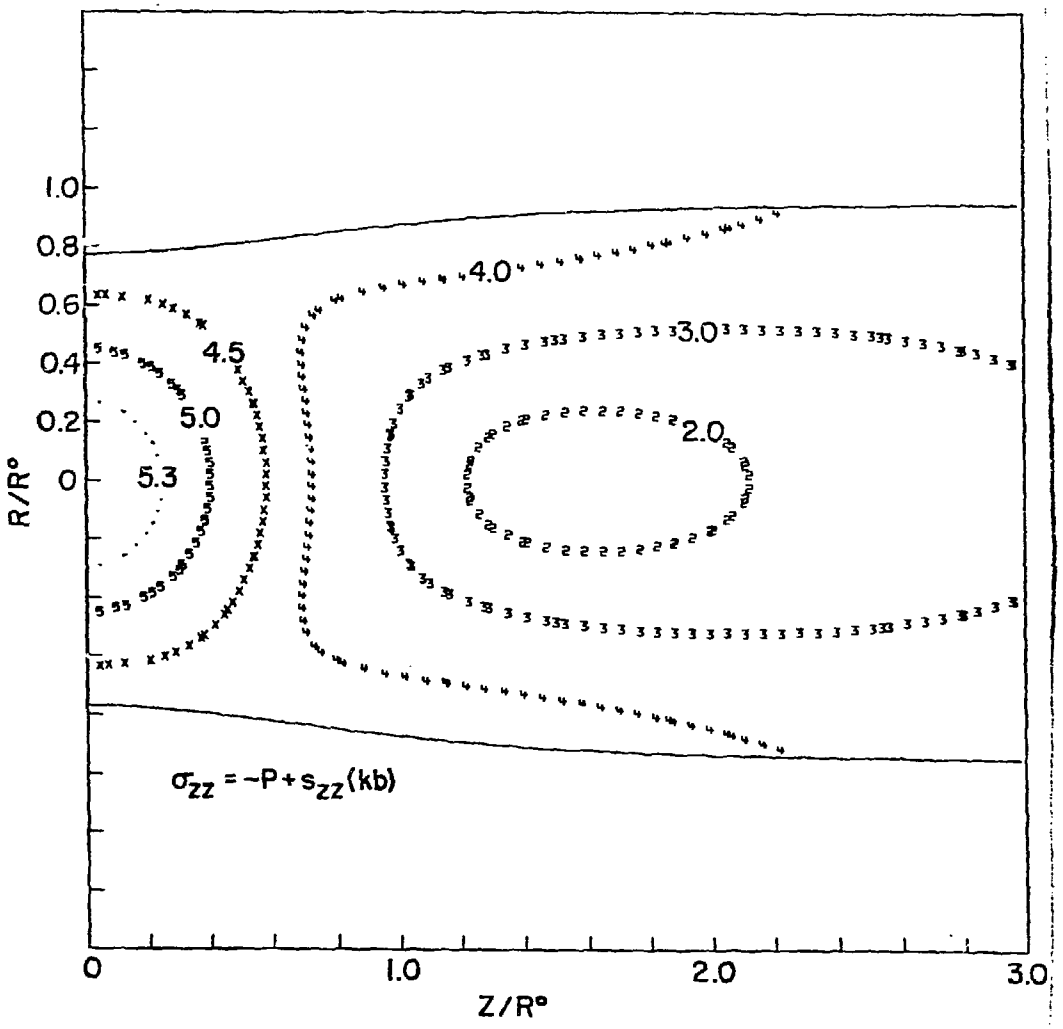

Figure 5 Calculated contours of axial stress σ_{zz} at time of fracture.

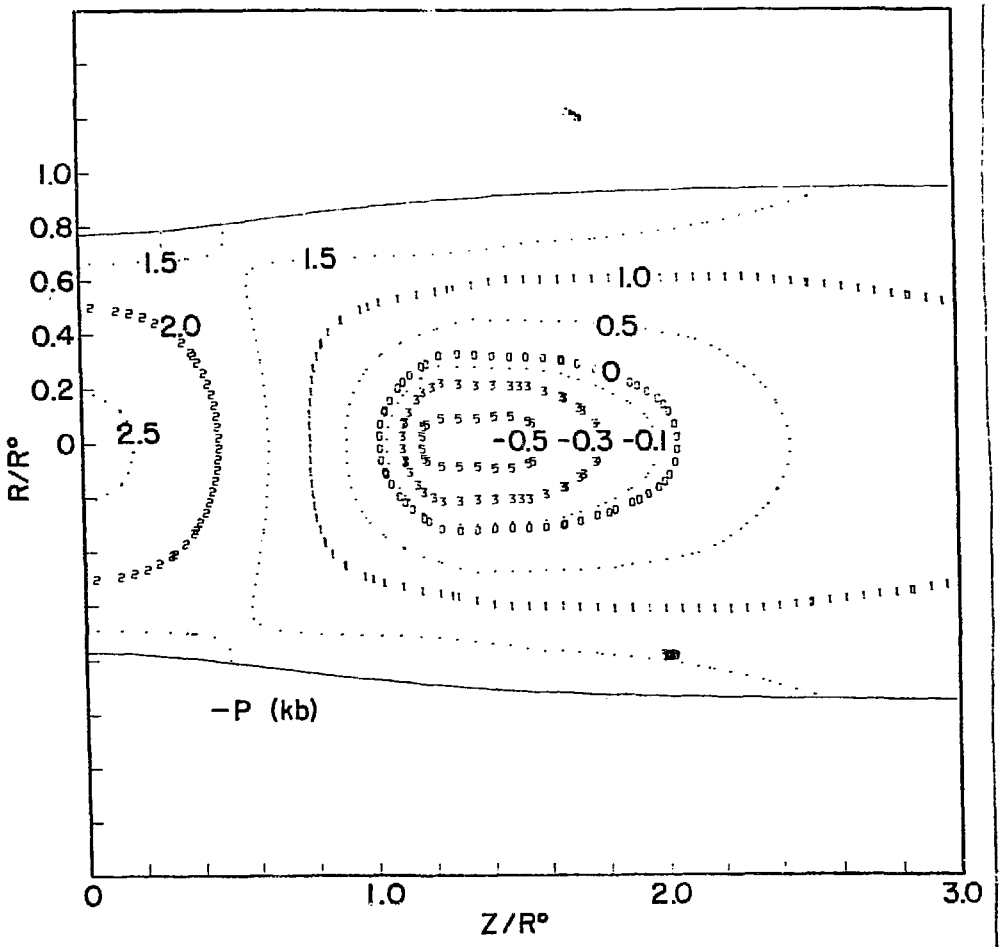

Figure 6 Calculated contour of the hydrostatic stress -P at time of fracture.

Application to Impact Experiments

The impact of a cylinder against a rigid boundary provides a simple geometry, to examine the behavior of the constitutive model for a different stress strain history. Figure 7 shows results of calculations and experiments for the impact of aluminum 6061 T6 cylinders against a rigid boundary. The experimental rigid boundary is obtained by backing a 1" thick tile of alumina with a 1" thick section of hard steel. The final lengths of the cylinders are very sensitive to the flow stress. All of the details of the experimental results were closely reproduced by the calculations using the constitutive model described.

At higher impact velocities the effect of temperature will become important. Additional experiments would be required to map out the regions of thermal softening. When the melting temperatures is reached the flow stress Y must be set to zero

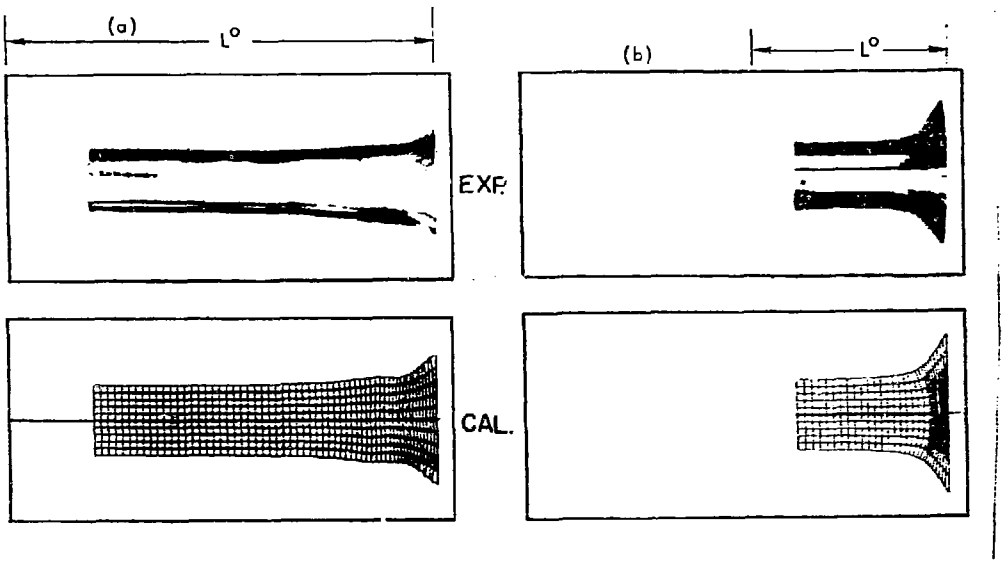

Figure 7 Comparison of experiment and calculation of right circular aluminum cylinders after striking a rigid boundary.

(a)	L_f^o = 4.69 cm	Original length	(b)	L_f^o = 2.35 cm
	L^f = 3.86 cm	Final length		L^f = 1.65 cm
	U = 0.0275 cm/sec	Impact velocity		U = 0.0373 cm/sec

Summary

The computer simulation of a simple tension test shows that the average values of stress and strain at a cross-section correspond well to the values obtained from external measurements. Thus external measurements of load and radial strain can be used to estimate a form that describes the flow stress as a function of equivalent plastic strain. The calculation is then checked with the experimental true stress, radial strain data. In general, it would be expected that several iterations of the flow stress function would be required before satisfactory agreement with the experimental data is obtained. In the example given here, a power law was found with a single calculation that provided close agreement between calculation and experiment . Care must be taken that fracture has not occurred in the range of data used to develop the flow stress function.

Acknowledgements

The simple tension test experiments were performed by Manuel Prado and the HEMP calculations were done by Nora Anson.

References

1. Wilkins, M. L., "Calculations of Elastic Plastic Flow", UCRL-7322, Rev. I, 1969.

2. Wilkins, M. L., Blum, R. E., Cronshagen, E. and Grantham, P., "A Method for Computer Simulation of Problems in Solid Mechanics and Gas Dynamics in Three Dimensions and Time", UCRL-51574, Rev. I, 1975.

3. Liang, W. K., Azou, P. and Bastien, P. , Les Mémoires Scientifiques de la Revue de Métallurgie, Janvier 1964, No. 1.

4. Wilkins, Mark L., Third Progress Report of Light Armor Program, July 9, 1968.

5. Norris, D., Wilkins, M., Moran, B., Prado M., Scudder, J., Quinones, D. and Reaugh, J., "Fundamental Study of Crack Initiation and Propagation", EPRI Research Project RP603-1, Annual Progress Report, 15 March 1976 to 15 March 1977, UCRL-52296.

Distribution

M. L. Wilkins (10)

TID (15)

External

S. S. Hecker
LASL
Co-Chairman of the TMS-AIME Shaping and Forming Committee